Aerospace Science and Technology 122 (2022) 107409

Contents lists available at ScienceDirect

Aerospace Science and Technology

www.elsevier.com/locate/aescte

A numerical study of oblique detonation re-stabilization by expansion waves

Kepeng Yao [a,b], Chun Wang [a,b,*], Zonglin Jiang [a,b]

[a] State Key Laboratory of High Temperature Gas Dynamics, Institute of Mechanics, Chinese Academy of Sciences, Beijing 100190, China
[b] School of Engineering Sciences, University of Chinese Academy of Sciences, Beijing 100049, China

ARTICLE INFO

Article history:
Received 7 June 2021
Received in revised form 7 December 2021
Accepted 8 February 2022
Available online 11 February 2022
Communicated by Yu Lv

Keywords:
Oblique detonation
Stationary
Thermal choking
Expansion waves

ABSTRACT

Oblique detonation engines have significant potential as air-breathing propulsion units because they can undergo self-ignition while providing high combustion efficiency. A key design aspect of such engines is the formation of a stationary oblique detonation wave in the combustor. In the present work, the re-stabilization of oblique detonation by expansion waves induced using a finite wedge was simulated by solving Euler equations in conjunction with an induction-exothermic kinetics model. The numerical results showed that expansion waves interacting with the subsonic region behind the unstable oblique detonation wave can produce a stationary oblique detonation wave on the wedge by eliminating thermal choking. The initiation position was also found to move downstream with decreases in wedge length, while the location of the expansion waves moved upstream. And the critical locations of expansion waves that re-stabilize and initiate an oblique detonation wave were also proposed. A special field structure that comprising two parts separated by unburned gas was observed at the incident Mach number $M_0 = 7.5$ when the expansion waves located near initiation critical location. The upper and lower parts comprised the detonation and deflagration fields, respectively. In others, the interaction of expansion waves leads to a smaller total pressure loss, so that is beneficial to improve the performance of oblique detonation engine in theory.

1. Introduction

Air-breathing hypersonic propulsion based on controlled combustion in conjunction with a high-speed inflow of air can be achieved using oblique detonation waves (ODWs). This newer type of engine is referred to as a shock-induced combustion ramjet (Shcramjet) or oblique detonation engine (ODE) [1,2] and has been widely studied over the past several decades. Early research typically represented the ODW as a simplified oblique shock wave (OSW) with instantaneous heat release and performed analyses based on shock theory [3,4]. Later work demonstrated the formation of an initiation region prior to the ODW surface that modifies the ODW structure [5,6]. Various investigations of ODW structures [7–13] were subsequently conducted using different chemical reaction models and demonstrated that a number of distinct wave structures were possible. A recent experimental study [14] verified these simulated structures and achieved steady combustion while producing a typical ODW wave structure.

A stable ODW structure is critical to developing a practical ODE having a finite wedge and variable inflow. Investigations of ODWs induced by a finite wedge have shown that the effect of expansion waves generated by the wedge corner may change the initiation pattern from an abrupt to a smooth transition [15]. The corner angle has also been found to play an important role in an ODW engine with a low intake velocity [16]. The interaction between the ODW and expansion waves induced by the upper wall corner results in a new wave configuration characterized by a post-turning triangular recirculation zone coupled with a gaseous wedge connecting the deflection point and the ODW surface [17,18]. Stable, critical or unstable structures can result, depending on the relative location of the wave reflection and the turning point of the upper wall [19]. The ODW surface has also been found to be unstable and to have the potential to become cellular even with a uniform inflow [20–24]. It is also possible for triple wave point structures to form on the ODW front. Other research has indicated that the appearance of this triple wave structure is affected by the activation energy of the combustible mixture [25], although

* Corresponding author at: State Key Laboratory of High Temperature Gas Dynamics, Institute of Mechanics, Chinese Academy of Sciences, Beijing 100190, China.
E-mail address: wangchun@imech.ac.cn (C. Wang).

https://doi.org/10.1016/j.ast.2022.107409
1270-9638/

determining the cellular structure requires numerical simulations with sufficient spatial resolution [26]. In the case of unsteady inflow with continuous disturbances, a progression through quasi-steady, oscillating and unstable ODW regimes has been identified with increases in the disturbance wave number [27]. These disturbances have also been shown to result in two types of triple wave point formations [28]. Research has demonstrated the concept of a critical incident M_0 value, M_{0cr}, below which the ODW induced by the wedge is unsteady, meaning that the initiation structure oscillates within a specific range [29]. Further decreases in the incident M_0 cause the ODW to travel upstream and detach.

The present work simulated an ODW generated using a finite wedge and assessed variations in the wave structure resulting from expansion waves. In contrast to previous studies [15,25,30], the numerical parameters employed herein were selected to model unsteady ODWs that traveled upstream without expansion waves. Notably, the wedge angle is less than the critical detached value. Unstable detonation's presence is mainly originated from the interactions of pressure wave and detonation front [31]. These original unsteady waves were found to re-stabilize themselves following the inclusion of expansion waves, and the various structural variations associated with this process are discussed and analyzed in this paper. The finite wedge used in this work was a simplified model of a combustion chamber and nozzle, and this study demonstrates that a steady ODW can be realized at a relatively low incident M_0, thus facilitating the ODE design process.

2. Physical and mathematical methods

A diagram of an ODW induced by a finite wedge in a pre-mixed combustible gas is shown in Fig. 1. In the case of supersonic inflow, the finite wedge initially generated an OSW. The temperature of the combustible gas behind this shock wave was sufficient to initiate an exothermic chemical reaction that in turn generated the ODW. For post-shock mixture, the exothermic reaction index λ will increase from 0 to 1 along the wedge. This current work focuses on the effect of expansion waves on the exothermic reactions. To determine the position of wedge corner that is used to trigger an expansion fan, a chemical parameter λ_w is defined in this study. The reaction fronts (red curves) are connected with the lower wedge surface. When one reaction front is located on the wedge corner, the reaction index of related reactive front is recorded as λ_w, as shown in Fig. 1.

Ng et al. previously proposed a two-step induction-exothermic kinetics model for chemical reactions [32] that has been adopted widely in simulations of ODWs [15,17,19,27–29,33]. This kinetic model is a general class of overall reaction mechanism. In previous studies [24,34–36], this kind of model is used in two ways. One is to reduce detailed reaction mechanism and improve computational efficiency for complex phenomena. Another target is to study the complex structures of heat release zone, in which the flow structures can be adjusted via varying some key chemical parameters. The current work focuses on the interaction of expansion waves and heat release process near initiation zone. This model used in this study involves two reaction process factors that could control heat release evolution of one detonation wave, which is convenient to the target of this work. Two-dimensional Euler equations based on this same concept were subsequently used to model ODWs. In this two-step mechanism, variables ζ and λ denote the index of the induction and exothermic reactions, respectively. The governing equations are:

$$\frac{\partial \rho}{\partial t} + \frac{\partial \rho u_j}{\partial x_j} = 0, \tag{1}$$

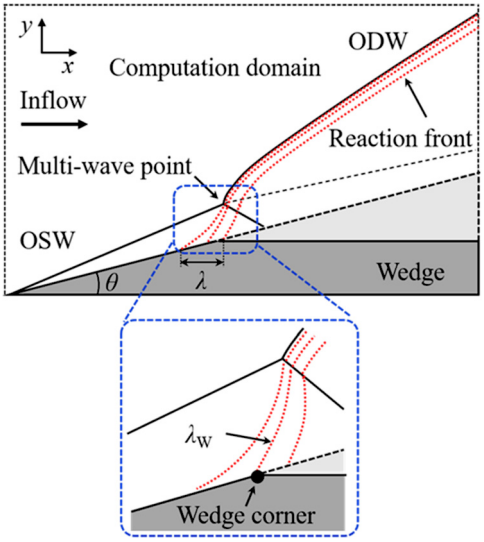

Fig. 1. Diagram of the wave complex with the computational domain. (For interpretation of the colors in the figure(s), the reader is referred to the web version of this article.)

$$\frac{\partial \rho u_i}{\partial t} + \frac{\partial \rho u_i u_j + p\delta_{ij}}{\partial x_j} = 0, \tag{2}$$

$$\frac{\partial \rho e}{\partial t} + \frac{\partial \rho u_j e + p u_j}{\partial x_j} = 0, \tag{3}$$

$$\frac{\partial \rho \xi}{\partial t} + \frac{\partial \rho \xi u_j}{\partial x_j} = \omega_\xi, \tag{4}$$

$$\frac{\partial \rho \lambda}{\partial t} + \frac{\partial \rho \lambda u_j}{\partial x_j} = \omega_\lambda, \tag{5}$$

$$\omega_\xi = H(1-\xi)\,\rho k_I exp\left[\frac{E_I}{R}\left(\frac{1}{T_s} - \frac{1}{T}\right)\right] \tag{6}$$

and

$$\omega_\lambda = [1 - H(1-\xi)]\,\rho(1-\lambda)\,k_R exp\left(\frac{-E_R}{RT}\right), \tag{7}$$

where E_I and E_R are the activation energies of the induction and exothermic reactions, respectively. The other variables shown here include the Heaviside step function, H, given by:

$$H(1-\xi) = \begin{cases} 1 & \xi < 1 \\ 0 & \xi \geq 1 \end{cases} \tag{8}$$

as well as

$$p = \rho RT \tag{9}$$

and

$$e = \frac{RT}{\gamma - 1} + \frac{u_j u_j}{2} + (1-\lambda)\,Q, \tag{10}$$

where δ_{ij} is the Kronecker variable. In addition, the variables ρ, u_j, e, T, p, γ, R and Q are density, velocity in the j direction, specific total energy, temperature, pressure, ratio of specific heat, gas constant and total chemical energy available in the mixture, respectively. All the variables are dimensionalized by the reference to uniform unburn state as follows:

$$\rho = \frac{\overline{\rho}}{\rho_0}, \quad p = \frac{\overline{p}}{p_0}, \quad T = \frac{\overline{T}}{T_0}, \quad u_j = \frac{\overline{u}_j}{\sqrt{R_0 T_0}}, \quad R = \frac{\overline{R}}{R_0}. \tag{11}$$

Where the variables with subscript '0' are unburn state parameters, and with superscript '-' are local variables of flow field. The

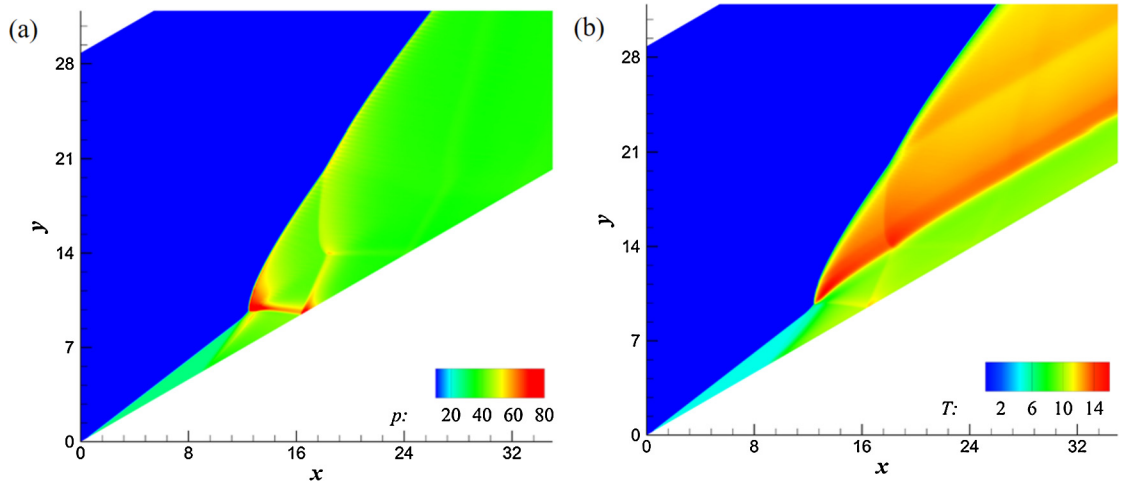

Fig. 2. (a) Pressure and (b) temperature fields for $M_0 = 8.0$.

parameters k_I and k_R are the pre-exponential factors for the induction and exothermic reactions, respectively. In this work, k_I = -U_{VN}, where U_{VN} is the post shock particle velocity in the shock fixed frame for the corresponding Chapman–Jouguet (C-J) detonation, with the induction length of the C-J detonation having a fixed value of unity. It can be calculated by the equations (12) & (13), where the M_{CJ} denote the C-J detonation wave velocity. The main parameters were set as $Q = 20.0$, $E_I = 10.0T_s$, $E_R = 1.0T_s$, $k_R = 7.0$, $\gamma = 1.32$ and $R_0 = 397.6$ J/(kg·K), where T_s is the post-shock temperature of the C-J detonation.

$$U_{VN} = \sqrt{\gamma} \times \frac{2 + (\gamma + 1) M_{CJ}^2}{(\gamma + 1) M_{CJ}^2} \tag{12}$$

$$M_{CJ}^2 = \left(1 + \frac{\gamma^2 - 1}{\gamma} Q\right) + \left[\left(1 + \frac{\gamma^2 - 1}{\gamma} Q\right)^2 - 1\right]^{\frac{1}{2}} \tag{13}$$

The governing equations were discretized on Cartesian grids and the dispersion-controlled dissipative (DCD) schemes proposed by Jiang [37] together with the flux vector splitting method proposed by Steger and Warming [38] were adopted to solve the governing equations. The initial flow field was uniform. Outflow conditions extrapolated from the interior are implemented on the right boundary and lower boundaries before the wedge. Slip boundary condition modeled as a mirror symmetry condition is applied at the wedge surface. The incoming boundaries condition with the fixed parameters are implemented on the left and upper boundaries. The computational domains were carried out using dimensionless length 50×40 and 120×100 for $M_0 = 7.5$ and 7.0, respectively. The wedge angle, θ, had a fixed value of 30°.

3. Results and discussion

3.1. Wave structures without expansion waves

The baseline case of $M_0 = 8.0$ was simulated and the results are presented in Fig. 2. In this simulation, the wedge began at $x = 0.5$, at which point the OSW was induced. It is evident that the OSW transitioned to an ODW via a triple wave point at approximately $x = 12$, corresponds to an abrupt initiation to the ODW. The transverse shock wave inside the ODW subsequently interacted with the wedge and was reflected. The reflected transverse shock wave then interacted with the slip line and formed a transmission shock wave that interacted with the ODW downstream. Two slip lines

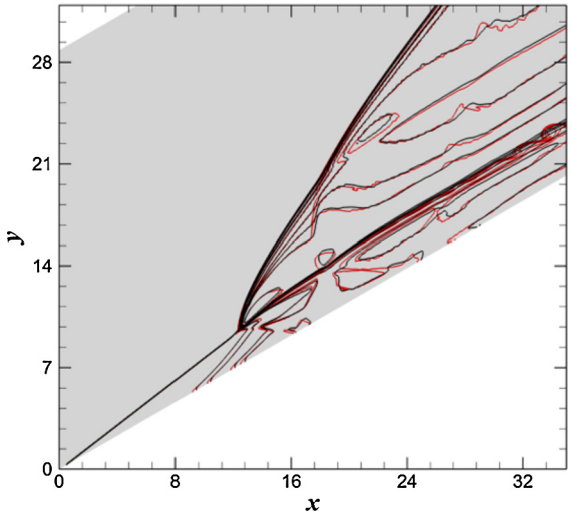

Fig. 3. Temperature contours generated with different grids for $M_0 = 8.0$. Red and black lines denote a grid resolution of 0.025 and 0.05, respectively.

are apparent, both of which are almost parallel to the wedge surface.

The effect of grid resolution was assessed by simulating ODW fields using different resolutions. Mean grid scales of 0.05 and 0.025 were used for this purpose, corresponding to 20 and 40 grid units over the induction length of the C-J detonation, respectively, and the resulting temperature contours are shown in Fig. 3. Here, the red and black lines indicate high and low resolution temperature contours, respectively, and the two types of lines are seen to almost coincide. The effect of resolution was examined by performing an additional quantitative comparison. In this exercise, the distributions of pressure and temperature along the wedge surface and along two lines parallel to the x-axis at $y = 20$ and 25 were extracted, as presented in Fig. 4. The distributions of temperature and pressure along the wedge surface are plotted in Fig. 4(a) while those along $y = 20$ and 25 are plotted in Fig. 4(b). Here, the solid and dashed red lines indicate the pressure and temperature distributions obtained using a grid scale of 0.025, respectively, while black lines show the data acquired with a grid scale of 0.05. The different color curves are seen to almost overlap. Thus, in the present study, a grid resolution of 0.05 was used to simulate ODWs as a means of balancing the computational complexity with simulation accuracy. Based on the above analysis, this choice is believed to have been reasonable.

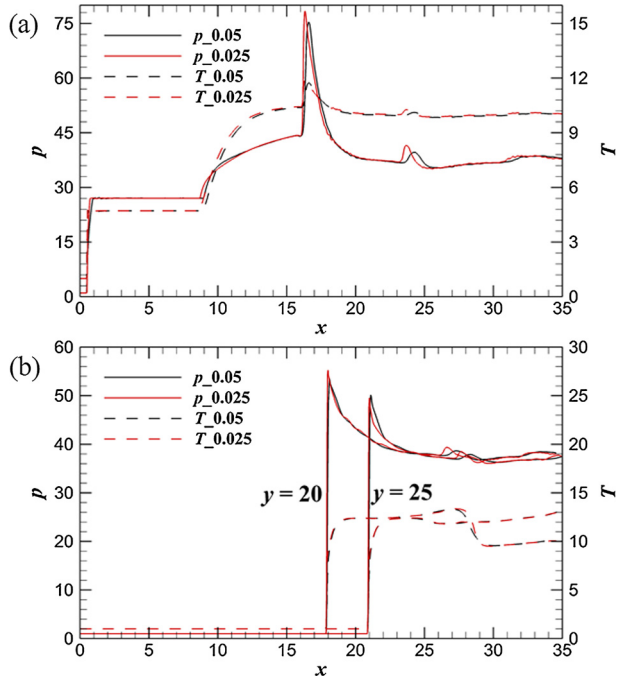

Fig. 4. Pressure and temperature distributions in the flow field (a) along the wedge and (b) along the lines of $y = 20$ and 25.

The ODW was found to become unsteady when the inflow Mach number was decreased to $M_0 = 7.5$ and 7.0, and the structure and dynamics of these two cases are provided in Fig. 5. $M_0 = 7.5$ generated an abrupt transition such that the transverse shock wave inside the ODW interacted with the wedge to form a Mach stem at $t = 15.1$. At $t = 63.1$, the ODW traveled upstream and the Mach stem was elongated while, at $t = 95.0$, the ODW traveled upstream continuously but the Mach stem disappeared. Notedly, at $t = 126.9$, the ODW initiation location moved downstream relative to the position at $t = 95.0$. It can be concluded that the ODW initiation location oscillated, as shown in Fig. 5(a). This structural evolution process was also studied by Yang [29], who found that the initiation structure was transient and oscillated around the equilibrium position. In the case of $M_0 = 7.0$, the ODW was initiated at $t = 32.6$ with a complex structure. The secondary detonation wave interacted with the transverse shock wave to generate a Mach stem, resulting in a normal detonation wave (NDW), while the secondary transverse shock wave interacted with the wedge surface to form a Mach stem. Over time, the ODW traveled upstream and the NDW first became longer then shortened until it disappeared, as shown in Fig. 5(b). Notedly, the ODW initiation location also oscillated in the case of $M_0 = 7.0$, although the oscillation amplitude was smaller than that obtained with $M_0 = 7.5$.

3.2. Effects of expansion waves on oblique detonation stability

The instability of shock wave induced combustion for a wedge with a flow turning angle greater than the maximum attach angle of oblique detonation wave was reported in Choi et al. [39]. And they revealed three different regimes of combustion through compared the chemical time behind OSW and NSW and fluid dynamic time, i.e., decoupled combustion, oscillatory combustion and detached overdriven detonation wave, respectively. However, the method and mechanism of re-stabilization unstable ODW has not been reported in previous study. In this current work, a re-stabilization approach of unstable ODWs is proposed. That is using expansion waves eliminated the thermal choking so that make the detonation wave standing on the wedge. These expansion waves were introduced by inserting a finite length wedge having a turning angle downstream, after which the outflow turned such that it was parallel to the inflow. Note that, in this study, the downstream turning angle was set equal to the wedge angle for simplicity, and more work is needed to clarify the effects of the downstream angle. The position of the expansion waves was selected as the reaction index of heat release at the corner. The reaction index of heat release on the corner was selected as the position of expansion waves.

The formation of a stationary ODW on the wedge were controlled by finite wedges with different lengths in the simulations. Fig. 6 demonstrates the ODW temperature fields obtained with a finite wedge for which $\lambda_w = 0.4$ using $M_0 = 7.5$ and 7.0. It is apparent that the ODW was stationary on the wedge surface and the initiation pattern involved an abrupt transition in both cases. Importantly, the initiation structure was different for the two M_0 values. Using $M_0 = 7.0$, the ODW was initiated in conjunction with a triple wave point and an NDW was observed, while the interaction between the transverse shock wave and the wedge formed a Mach stem. In contrast, neither an NDW nor a Mach stem appeared using $M_0 = 7.5$. It is concluded that the presence of expansion waves would be expected to affect the oblique detonation stability.

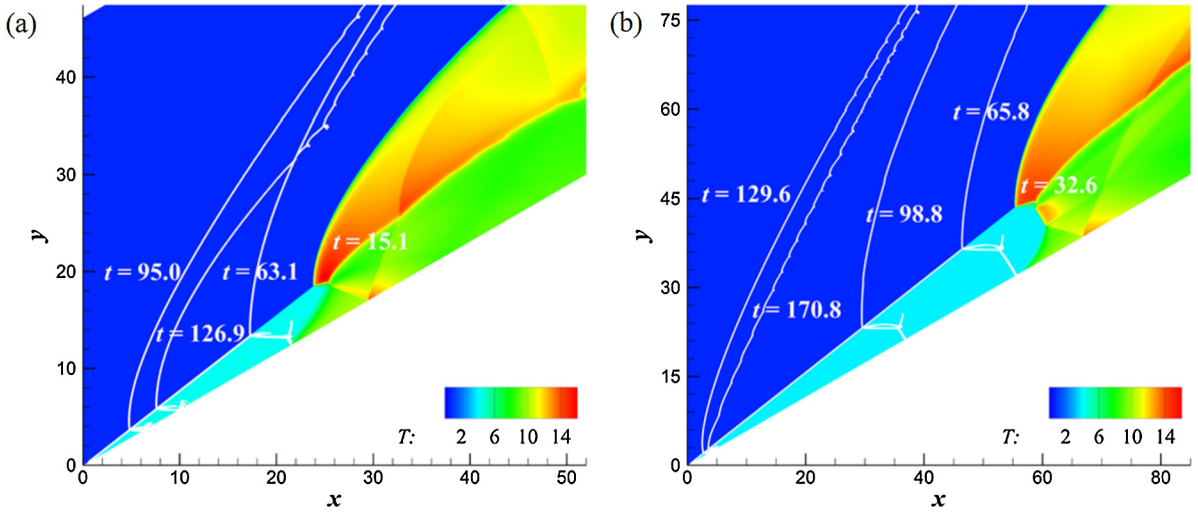

Fig. 5. Temperature fields for (a) $M_0 = 7.5$ and (b) $M_0 = 7.0$. White curves denote OSW and ODW fronts at different times.

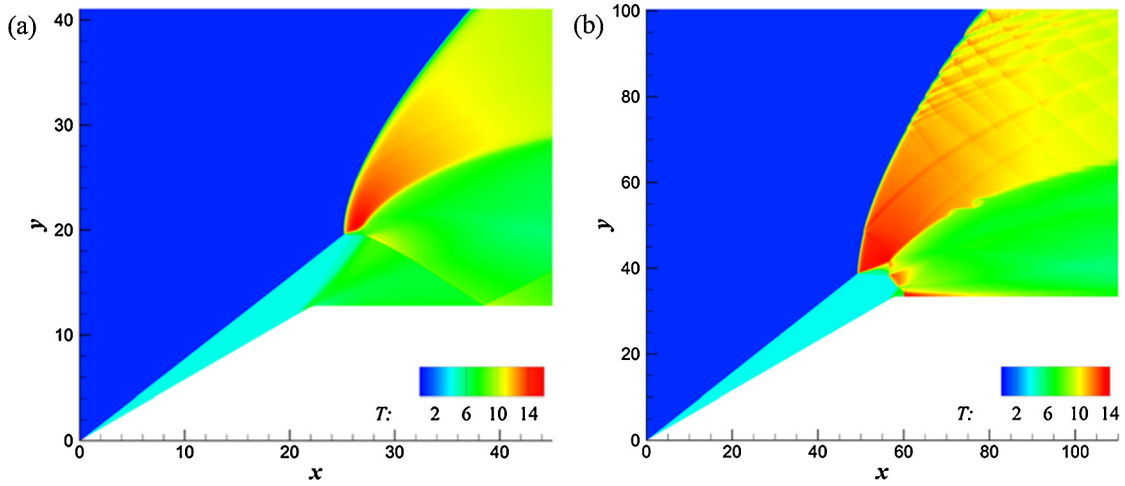

Fig. 6. Temperature contours of re-stabilization oblique detonation wave fields obtained with different inflow conditions and wedge length L: (a) $\lambda_w = 0.4$ ($L = 25$), $M_0 = 7.5$ and (b) $\lambda_w = 0.4$ ($L = 66$), $M_0 = 7.0$.

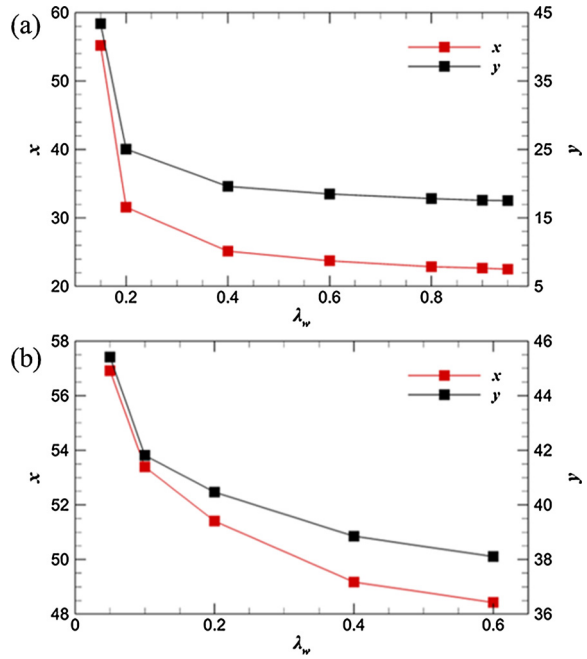

Fig. 7. Initiation locations (x in (x, y)) as functions of λ_w for (a) $M_0 = 7.5$ and (b) $M_0 = 7.0$.

The effects of the expansion waves location on the ODW initiation location and structure were assessed by performing additional simulations with various λ_w. The initiation locations are plotted as functions of λ_w in Fig. 7, which indicates that the location moved downstream as λ_w was decreased. From Fig. 7(a), it is also evident that the initiation location was more sensitive to the position of the expansion waves at lower λ_w. Notably, for $0.15 < \lambda_w < 0.95$, an ODW was initiated and stationary on the wedge surface, while a λ_w value of 0.99 (data not shown) gave a non-stationary initiation structure such that the ODW traveled upstream. Decreasing λ_w to 0.10 meant that an ODW could not be initiated, although a combustion zone was observed. Thus, there were two critical values, those being $\lambda_{wL} = 0.10 - 0.15$ and $\lambda_{wU} = 0.95 - 0.99$, for which, if $\lambda_w < \lambda_{wL}$, the ODW could not be initiated while, if $\lambda_w > \lambda_{wU}$, the ODW was detached. From Fig. 7(b), it can be seen that, for $M_0 = 7.0$, the ODW initiation location moved downstream with decreases in λ_w, similar to the case of $M_0 = 7.5$. For $0.05 < \lambda_w < 0.60$, an ODW was initiated and stationary on the wedge surface. An increase to $\lambda_w = 0.65$ initiated an ODW but this ODW was detached. Evidently, there was a critical value, that being $\lambda_{wU} = 0.60 - 0.65$, for which, when $\lambda_w > \lambda_{wU}$, the ODW was detached. Upon decreasing λ_w to 0, the ODW could not be initiated and there was a critical value of $\lambda_{wL} = 0 - 0.05$, for which, when $\lambda_w < \lambda_{wL}$, the ODW could not be initiated. The critical values λ_{wL} and λ_{wU} were smaller for $M_0 = 7.0$ than for $M_0 = 7.5$, indicating that the expansion waves had a greater impact on the ODW at larger incident Mach numbers.

Prior research [15] has shown that the expansion waves induced by the corner of the wedge may change the ODW initiation pattern from an abrupt to smooth transition. However, in the present work the use of $M_0 = 7.5$ and 7.0 did not indicate changes in the initiation pattern in response to expansion waves, although a special wave structure was obtained for $M_0 = 7.5$. The temperature and heat release rate contours obtained using $M_0 = 7.5$ and $\lambda_w = 0.15$ are provided in Fig. 8, and it can be seen that the flow field was separated into two parts by a region in which there was no reaction (Fig. 8(a)). Fig. 8(b) demonstrates the heat release rate field associated with the critical conditions, with the shock wave front indicated by the white line. These data confirm that the exothermic reaction and shock wave were decoupled in the lower side of the non-reactive region but were tightly coupled in the upper side. Thus, the upper and lower parts represented the detonation and deflagration fields. Many triple wave point structures are apparent on the detonation wave, although these structures are different from the ODW wave front obtained at $M_0 = 7.0$ as shown in Fig. 6(b). In the case of this critical structure, the detonation wave front was found to be unstable. In contrast, this special structure was not observed using $M_0 = 7.0$.

3.3. The ODW re-stabilization mechanism

The prior section discussed the effect of expansion waves on oblique detonation stability, and described a special structure in which the field was separated into two parts by unburned gas based on the interaction of expansion waves at $M_0 = 7.5$. Here, we discuss the oblique detonation re-stabilization mechanism. Two critical wave structures were observed in the case of $M_0 = 7.5$, comprising a stationary critical structure when $\lambda_w = 0.95$ and an initiation critical structure when $\lambda_w = 0.20$, as shown in Fig. 9. Here, the solid and dashed red lines represent the contours for $\lambda = 0.01$ and 0.99, respectively, and the sub-sonic region surrounded by the dashed blue curves indicates the contour line for $Ma = 1.0$. From Fig. 9(a), it is evident that a standard, abrupt

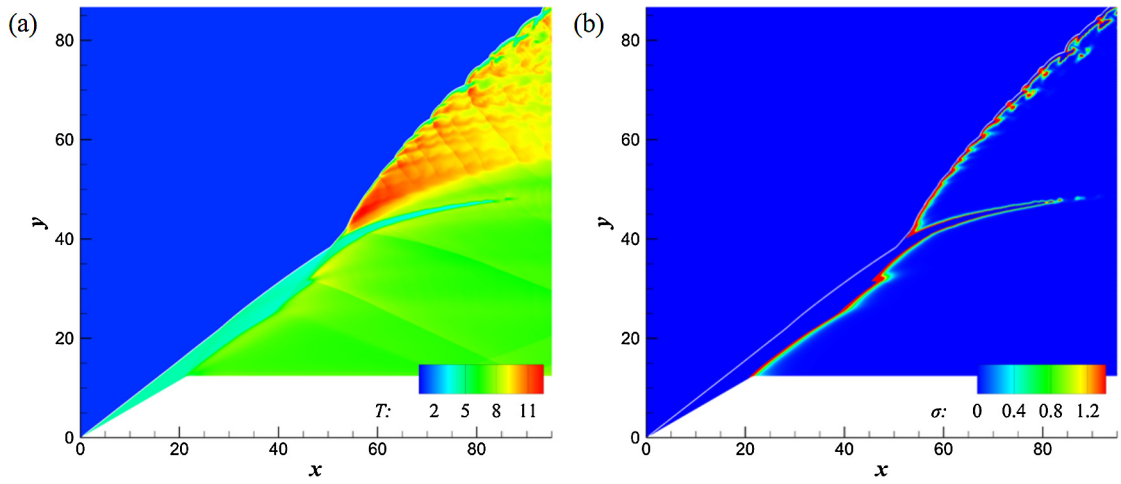

Fig. 8. (a) Temperature and (b) heat release rate contours of the flow fields in the case of $M_0 = 7.5$ and $\lambda_w = 0.15$. The white curve denotes the shock wave front.

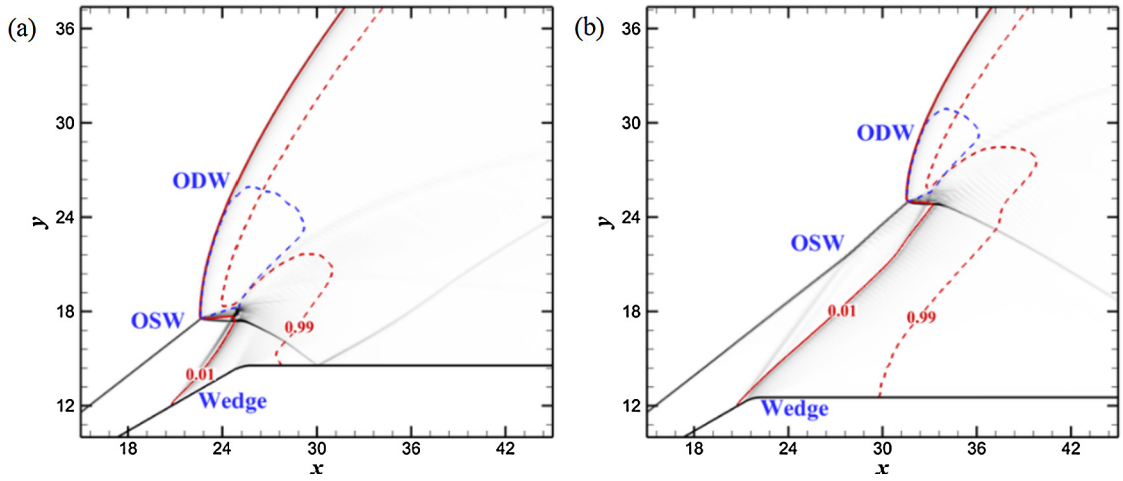

Fig. 9. Density gradient fields in the case of $M_0 = 7.5$ with (a) $\lambda_w = 0.95$ and (b) $\lambda_w = 0.20$. The solid and dashed red lines indicate $\lambda = 0.01$ and 0.99, respectively, while the blue lines denote the sonic location.

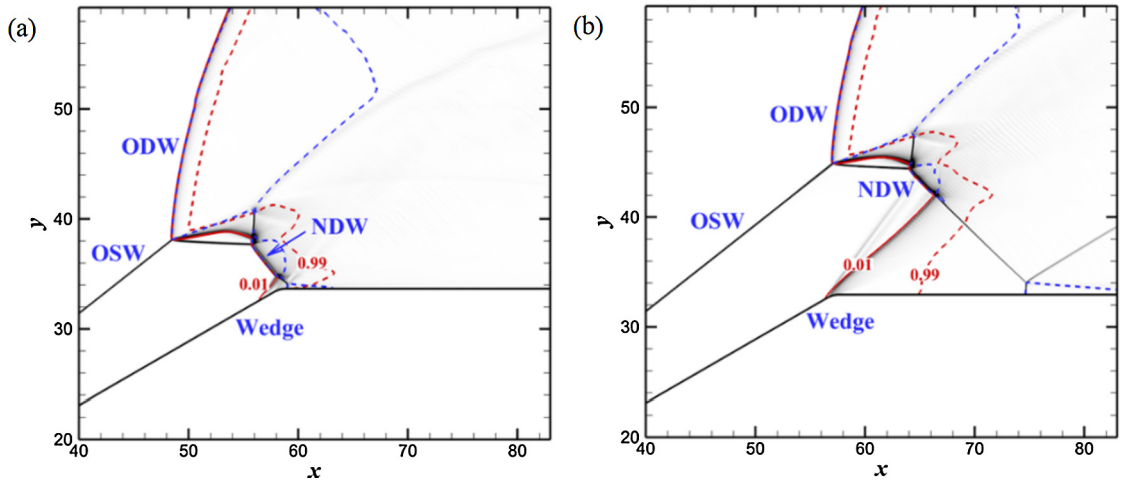

Fig. 10. Density gradient fields obtained with $M_0 = 7.5$ for (a) $\lambda_w = 0.60$ and (b) $\lambda_w = 0.05$. The solid and dashed red lines indicate $\lambda = 0.01$ and 0.99, respectively, while the blue lines denote the sonic location.

initiation structure was obtained and that the OSW transitioned to an ODW with a triple wave point. In addition, the transverse shock wave was distorted as it interacted with the deflagration wave and then with the wedge surface. Fig. 9(b) demonstrates that the initiation structure was similar to that obtained using $\lambda_w = 0.95$ (Fig. 9(a)), but the initiation position was located further downstream. Fig. 10 shows that two critical wave structures were formed in the case of $M_0 = 7.0$: a stationary critical structure at $\lambda_w = 0.60$ and an initiation critical structure at $\lambda_w = 0.05$. It is apparent that the initiation structure was different from the

standard abrupt structure, and was made up of a more complicated wave system. The ODW was initiated in conjunction with a triple wave point and the transverse shock wave interacted with the secondary detonation wave to form a Mach stem that resulted in an NDW. In addition, another transverse shock wave interacted with the wedge surface to generate another Mach stem, as shown in Fig. 10(a). In this figure, the solid and dashed red lines indicate the contours of the exothermic reaction variable, λ, with values of 0.01 and 0.99, respectively, that denote the start and end of the exothermic reaction. The dashed blue curves denote the sonic location, as in Fig. 9. The initiation structures in Fig. 10(a) and 10(b) are similar, but the initiation position is further downstream in the latter, indicating that the expansion waves had little effect on the initiation structure. It should be noted that three subsonic regions were identified, enclosed by the dashed blue lines behind the two Mach stems and the oblique detonation in both cases at $M_0 = 7.0$, while just one region appeared behind the initiation point of the oblique detonation in the case of $M_0 = 7.5$ (Fig. 9).

The ODW angle was very large in conjunction with an abrupt transition initiated by a triple wave point, meaning that the degree of overdriving of the ODW was also very large. In addition, a sub-sonic region was formed as the flow was highly compressed by the ODW. The sub-sonic region grew larger along with the evolution of the ODW and the thermal choking effect moved the ODW upstream. The expansion waves induced by the corner interacted with the sub-sonic region behind the ODW to decrease the strength of the ODW in the initiation region and eliminate thermal choking. These effects produced a stationary ODW on the wedge.

This paper proposed a method that re-stabilization unstable ODW using expansion waves. And whether the expansion waves decline the efficiency of ODE would be discussed here. In ODE, the combustor exit is connected with the engine nozzle. The interaction of expansion waves induced by secondary downstream wedge and detonation front is inevitable in realistic engine. Since the self-propagating features of gaseous detonation wave, the ODW could maintain a specific value in theory where the normal velocity of free inflow is equal to the CJ detonation velocity of the corresponding mixture. Its over-driven degree is 1.0 [40]. However, for the design of ODE, the wedge angle is design to larger than the CJ wedge angle so that ODW can be initiated by finite wedge, so as the over-driven degree is larger than 1.0. According to gas-dynamic theory, larger over-driven degree will cause a significant loss in total pressure of inflow and reduce the efficiency of ODE. Notably, the interaction of expansion waves induced by the wedge will decrease the over-driven degree, i.e., it leads to a smaller total pressure loss. Hence, the expansion waves will improve the efficiency of ODE in theory. However, in combustor of ODE, there are recirculation zones and other complex structures, the combustion efficiency and performance of ODE needs further research.

4. Conclusions

ODWs induced by the presence of a finite wedge were simulated by solving Euler equations together with a two-step induction-exothermic chemical reaction kinetics model. The parameters were chosen to correspond to unsteady ODWs, which traveled upstream without expansion waves. The ODW initiation position and stability characteristics were examined by employing different wedge lengths (that is, by varying λ_w). The numerical results suggested that the introduction of expansion waves may re-stabilize the ODW, and that the initiation position was sensitive to the location of expansion waves. Two critical values, λ_{wL} and λ_{wU}, were identified such that, with $\lambda_w < \lambda_{wL}$, an ODW could not be initiated. In addition, with $\lambda_w > \lambda_{wU}$, an ODW could not be re-stabilized, meaning that the ODW traveled upstream after being initiated. An ODW was both initiated and stationary on the wedge in the case of $\lambda_{wL} < \lambda_w < \lambda_{wU}$, while the initiation position moved downstream with decreases in λ_w. The critical values of λ_{wL} and λ_{wU} were found to decrease with increases in M_0. Decreasing λ_w to 0.15 generated a special structure such that the flow field was separated into two parts divided by unburned gas in the case of $M_0 = 7.5$, with the upper and lower sides representing the detonation and deflagration fields. However, this structure was not observed for $M_0 = 7.0$, meaning that the presence of expansion waves had a greater effect on the ODW initiation structure at higher M_0. And the expansion waves can decrease the over-driven degree of ODW, lead to a smaller total pressure loss, so that the expansion waves improve the efficiency of ODE in theory.

Declaration of competing interest

The authors declare that they have no known competing financial interests or personal relationships that could have appeared to influence the work reported in this paper.

Acknowledgements

The research is supported by the National Natural Science Foundation of China (Grant No. 11727901).

References

[1] J.P. Sislian, H. Schirmer, R. Dudebout, et al., Propulsive performance of hypersonic oblique detonation wave and shock-induced combustion ramjets, J. Propuls. Power 17 (3) (2001) 599–604.
[2] J. Urzay, Supersonic combustion in air-breathing propulsion systems for hypersonic flight, Annu. Rev. Fluid Mech. 50 (1) (2018) 593–627.
[3] D.T. Pratt, J.W. Humphrey, D.E. Glenn, Morphology of standing oblique detonation waves, J. Propuls. Power 7 (5) (1991) 837–845.
[4] S.A. Ashford, G. Emanuel, Wave angle for oblique detonation waves, Shock Waves 3 (4) (1994) 327–329.
[5] C. Li, K. Kailasanath, E.S. Oran, Detonation structures behind oblique shocks, Phys. Fluids 6 (4) (1994) 1600–1611.
[6] C. Viguier, L.F.F. da Silva, D. Desbordes, et al., Onset of oblique detonation waves: comparison between experimental and numerical results for hydrogen-air mixtures, Symp. (Int.) Combust. 26 (2) (1996) 3023–3031.
[7] H. Teng, H.D. Ng, Z. Jiang, Initiation characteristics of wedge-induced oblique detonation waves in a stoichiometric hydrogen-air mixture, Proc. Combust. Inst. 36 (2) (2017) 2735–2742.
[8] H. Teng, C. Tian, Y. Zhang, et al., Morphology of oblique detonation waves in a stoichiometric hydrogen–air mixture, J. Fluid Mech. 913 (2021) A1.
[9] Y. Fang, Y. Zhang, X. Deng, et al., Structure of wedge-induced oblique detonation in acetylene-oxygen-argon mixtures, Phys. Fluids 31 (2) (2019) 026108.
[10] Y. Zhang, Y. Fang, H.D. Ng, et al., Numerical investigation on the initiation of oblique detonation waves in stoichiometric acetylene–oxygen mixtures with high argon dilution, Combust. Flame 204 (2019) 391–396.
[11] C. Tian, H. Teng, H.D. Ng, Numerical investigation of oblique detonation structure in hydrogen-oxygen mixtures with Ar dilution, Fuel 252 (2019) 496–503.
[12] Z. Ren, B. Wang, Numerical study on stabilization of wedge-induced oblique detonation waves in premixing kerosene-air mixtures, Aerosp. Sci. Technol. 107 (2020) 106245.
[13] F.K. Lu, H. Fan, D.R. Wilson, Detonation waves induced by a confined wedge, Aerosp. Sci. Technol. 10 (8) (2006) 679–685.
[14] Z. Jiang, Z. Zhang, Y. Liu, et al., The criteria for hypersonic airbreathing propulsion and its experimental verification, Chin. J. Aeronaut. 34 (3) (2020) 94–104.
[15] G. Xiang, X. Gao, W. Tang, et al., Numerical study on transition structures of oblique detonations with expansion wave from finite-length cowl, Phys. Fluids 32 (5) (2020) 056108.
[16] Y. Fang, Z. Hu, H. Teng, Numerical investigation of oblique detonations induced by a finite wedge in a stoichiometric hydrogen-air mixture, Fuel 234 (2018) 502–507.
[17] K. Wang, H. Teng, P. Yang, et al., Numerical investigation of flow structures resulting from the interaction between an oblique detonation wave and an upper expansion corner, J. Fluid Mech. 903 (2020) A28.
[18] K. Wang, P. Yang, H. Teng, Steadiness of wave complex induced by oblique detonation wave reflection before an expansion corner, Aerosp. Sci. Technol. 112 (2021) 106592.
[19] K. Wang, Z. Zhang, P. Yang, et al., Numerical study on reflection of an oblique detonation wave on an outward turning wall, Phys. Fluids 32 (4) (2020) 046101.

[20] J. Verreault, A.J. Higgins, R.A. Stowe, Formation of transverse waves in oblique detonations, Proc. Combust. Inst. 34 (2) (2013) 1913–1920.
[21] L. Yang, L. Yue, Q. Zhang, et al., Numerical study on the shock/combustion interaction of oblique detonation waves, Aerosp. Sci. Technol. 104 (2020) 105938.
[22] Y. Zhang, L. Zhou, J. Gong, et al., Effects of activation energy on the instability of oblique detonation surfaces with a one-step chemistry model, Phys. Fluids 30 (10) (2018) 106110.
[23] Y. Zhang, L. Zhou, H. Meng, et al., Reconstructing cellular surface of gaseous detonation based on artificial neural network and proper orthogonal decomposition, Combust. Flame 212 (2020) 156–164.
[24] W. Han, C. Wang, C.K. Law, Three-dimensional simulation of oblique detonation waves attached to cone, Phys. Rev. Fluids 4 (5) (2019) 053201.
[25] M.V. Papalexandris, A numerical study of wedge-induced detonations, Combust. Flame 120 (4) (2000) 526–538.
[26] J. Choi, D. Kim, I. Jeung, et al., Cell-like structure of unstable oblique detonation wave from high-resolution numerical simulation, Proc. Combust. Inst. 31 (2007) 2473–2480.
[27] P. Yang, H.D. Ng, H. Teng, Numerical study of wedge-induced oblique detonations in unsteady flow, J. Fluid Mech. 876 (2019) 264–287.
[28] P. Yang, H.D. Ng, H. Teng, Unsteady dynamics of wedge-induced oblique detonations under periodic inflows, Phys. Fluids 33 (1) (2021) 016107.
[29] P. Yang, H. Teng, Z. Jiang, et al., Effects of inflow Mach number on oblique detonation initiation with a two-step induction-reaction kinetic model, Combust. Flame 193 (2018) 246–256.
[30] G. Xiang, X. Li, X. Sun, et al., Investigations on oblique detonations induced by a finite wedge in high altitude, Aerosp. Sci. Technol. 95 (2019) 105451.
[31] H. Teng, H.D. Ng, P. Yang, et al., Near-field relaxation subsequent to the onset of oblique detonations with a two-step kinetic model, Phys. Fluids 33 (9) (2021).
[32] H.D. Ng, M.I. Radulescu, A.J. Higgins, et al., Numerical investigation of the instability for one-dimensional Chapman–Jouguet detonations with chain-branching kinetics, Combust. Theory Model. 9 (3) (2005) 385–401.
[33] P. Yang, H. Teng, H.D. Ng, et al., A numerical study on the instability of oblique detonation waves with a two-step induction–reaction kinetic model, Proc. Combust. Inst. 37 (3) (2019) 3537–3544.
[34] H. Tofaili, G. Lodato, L. Vervisch, et al., One-dimensional dynamics of gaseous detonations revisited, Combust. Flame 232 (2021).
[35] K.C. Tang-Yuk, X.C. Mi, J.H.S. Lee, et al., Transmission of a detonation wave across an inert layer, Combust. Flame 236 (2022).
[36] C. Yan, H. Teng, H.D. Ng, Effects of slot injection on detonation wavelet characteristics in a rotating detonation engine, Acta Astronaut. 182 (2021) 274–285.
[37] Z. Jiang, On dispersion-controlled principles for non-oscillatory shock-capturing schemes, Acta Mech. Sin. 20 (1) (2004) 1–15.
[38] J.L. Steger, R.F. Warming, Flux vector splitting of the inviscid gas-dynamic equations with application to finite-difference methods, J. Comput. Phys. 40 (2) (1981) 263–293.
[39] J.Y. Choi, E.J.R. Shin, I.-S. Jeung, Unstable combustion induced by oblique shock waves at the non-attaching condition of the oblique detonation wave, Proc. Combust. Inst. 32 (2009) 2387–2396.
[40] H. Teng, Z. Jiang, H.D. Ng, Numerical study on unstable surfaces of oblique detonations, J. Fluid Mech. 744 (2014) 111–128.